Analyzing multiple spike trains with nonparametric granger causality

**Aatira G. Nedungadi · Govindan Rangarajan ·
Neeraj Jain · Mingzhou Ding**

Abstract Simultaneous recordings of spike trains from
multiple single neurons are becoming commonplace.
Understanding the interaction patterns among these spike
trains remains a key research area. A question of interest is
the evaluation of information flow between neurons
through the analysis of whether one spike train exerts
causal influence on another. For continuous-valued time
series data, Granger causality has proven an effective
method for this purpose. However, the basis for Granger
causality estimation is autoregressive data modeling, which
is not directly applicable to spike trains. Various filtering
options distort the properties of spike trains as point
processes. Here we propose a new nonparametric approach
to estimate Granger causality directly from the Fourier
transforms of spike train data. We validate the method on
synthetic spike trains generated by model networks of
neurons with known connectivity patterns and then apply it
to neurons simultaneously recorded from the thalamus and
the primary somatosensory cortex of a squirrel monkey
undergoing tactile stimulation.

1 Introduction

Advances in the hardware and computer technology have
made it comparatively easy to simultaneously record spike
trains from multiple single neurons. Such data can be
used to study how neurons interact with one another to
generate thought and behavior and how the cooperative
activity breaks down in disease (Brown et al. 2004).
Mathematically, neuronal spike trains are modeled as
stochastic point processes (Bartlett 1963; Rosenberg et al.
1989, 1998; Brillinger 1992; Halliday et al. 1995; Dahlhaus
et al. 1997; Brown et al. 2004). Although tools such as
cross correlation, coherence, partial correlation, and partial
coherence constitute the core of multiple spike train
analysis, they offer limited insights into how information
flows from one neuron to another. For continuous-valued
signals, e.g. EEG and local field potential (LFP), recent
work has shown that Granger causality is suited for this
purpose (Granger 1969; Baccala and Sameshima 2001;
Albo et al. 2004; Brovelli et al. 2004; Seth 2005; Chen
et al. 2006a, b; Ding et al. 2006; Wu et al. 2008). In
particular, directional information afforded by Granger
causality has played a pivotal role in generating testable
hypothesis regarding the function of cortical oscillatory
networks (Brovelli et al. 2004; Ding et al. 2006; Bollimunta
et al. 2008; Zhang et al. 2008). The effort to extend Granger
causality to point processes, however, faces considerable
challenges (Brown et al. 2004; Okatan et al. 2005; Truccolo
et al. 2005).

Granger causality is a statistical measure based on the
concept of time series forecasting. Specifically, if the

A. G. Nedungadi · G. Rangarajan (✉)
Department of Mathematics, Indian Institute of Science,
Bangalore 560 012, India
e-mail: rangaraj@math.iisc.ernet.in

N. Jain
National Brain Research Centre,
Manesar, Haryana 122050, India

M. Ding
J. Crayton Pruitt Family Department of Biomedical Engineering,
University of Florida,
Gainesville, FL 32611, USA

current state of a time series is better predicted by incorporating the past knowledge of a second one, the second series is said to have a causal influence on the first. The estimation of Granger causality relies on autoregressive (AR) models. For continuous-valued data such as EEG and LFP, AR model fitting is straightforward, and has been tested extensively with excellent outcome. For multivariate spike trains, AR modeling is not directly applicable. Recent work converts spikes trains into continuous time series by using a low pass filter or a smoothing kernel (Sameshima and Baccala 1999; Fanselow et al. 2001; Kaminski et al. 2001; Zhu et al. 2003). While this approach has been applied to both simulated and experimental data with generally acceptable results, it is cautioned that the smoothing operation violates the point process character of spike trains, and may introduce spurious effects (Truccolo et al. 2005).

The goal of this work is to present an alternative way of estimating Granger causality for point processes that is nonparametric and bypasses the step of autoregressive model fitting. The theoretical basis is three-fold: (1) the well-established spectral representation of point processes and its role in point process forecasting (Daley and Vere-Jones 2003, 2007), (2) factorization of spectral matrices (Wilson 1972), and (3) formulation of Granger causality in the spectral domain (Geweke 1982, 1984). Second-order statistical properties of multiple spike trains are summarized in the form of a spectral matrix (Rosenberg et al. 1989, 1998; Halliday et al. 1995; Dahlhaus et al. 1997; Jarvis and Mitra 2001; Brown et al. 2004). Combining spectral matrix factorization with Geweke's spectral formulation of Granger causality leads to the estimation of both pairwise and conditional Granger causality for multivariate point processes. We first tested the validity of the method by considering simulated spike train data and then applied it to data recorded simultaneously from the somatosensory cortical area 3b and the ventroposterior nucleus of the thalamus from a squirrel monkey (Jain et al. 2001) experiencing tactile stimulation.

2 Methods

2.1 Multivariate point processes and parameter estimation

Spikes are very brief in duration (~1 ms) and can be considered point events. A given spike train often has a random appearance and is treated as one realization of an underlying stochastic point process (Rosenberg et al. 1998). Let $N_1(t)$ be a counting variable denoting the number of spikes in the time interval $(0,t]$. The process $N_1(t)$ is said to be wide-sense stationary, mixing, and orderly, if (1) the statistical properties of the process are time-invariant, (2) the number of events occurring in intervals separated widely in time are independent, and (3) given a sufficiently small interval, the number of events in that interval is at most one (Conway et al. 1993; Halliday et al. 1995). The number of events in a small time interval dt is $dN_1(t) = N_1(t+dt) - N_1(t)$. Then $E\{dN_1(t)\} = P_1 dt$ where E stands for the expectation operator and

$$P_1 = \lim_{h \to 0} \Pr\{N_1 \text{ event in } (t, t+h)\} \Big/ h \tag{1}$$

Here P_1 is called the mean intensity of the process $N_1(t)$ (Conway et al. 1993; Halliday et al. 1995; Rosenberg et al. 1998). For theoretical and practical convenience the zero-mean process $N_1(t) - P_1 t$ will be considered henceforth and renamed $N_1(t)$ (Jarvis and Mitra 2001).

The spike trains generated by a group of m neurons are realizations of an m-dimensional multivariate stochastic point process. The vector counting variable is $\mathbf{N}(t) = (N_1(t), N_2(t), \ldots, N_m(t))^T$ where T stands for matrix transpose. The second-order cross-product density between the ith and jth components of N(t) at lag u is defined through the relation (Conway et al. 1993; Halliday et al. 1995; Rosenberg et al. 1998):

$$E\{dN_i(t+u)dN_j(t)\} = P_{ij}(u)dudt \tag{2}$$

where $P_{ij}(u)$ is defined as:

$$P_{ij}(u) = \lim_{h,h' \to 0} \Pr\{N_i \text{ event in } (t+u, t+u+h] \text{ and } N_j \text{ event in } (t, t+h']\} \Big/ hh' \tag{3}$$

The value of $P_{ii}(u)$ at $u=0$ is such that the above function is continuous at this point.

By considering the zero-mean process, the cross-covariance density function $q_{ij}(u)$ at lag u is (Conway et al. 1993; Halliday et al. 1995; Rosenberg et al. 1998):

$$\text{cov}\{dN_i(t+u), dN_j(t)\} = q_{ij}(u)dudt \tag{4}$$

where $q_{ij}(u)$ is related to the intensity functions for $u \neq 0$ by

$$q_{ij}(u) = P_{ij}(u) - P_i P_j. \tag{5}$$

For $i=j$, the auto-covariance density function turns out to be:

$$\text{cov}\{dN_i(t+u), dN_i(t)\} = (\delta(u)P_i + q_{ii}(u))dudt \tag{6}$$

where $\delta(u)$ is the classical Kronecker delta function.

For a single neuron the mean firing intensity can be estimated by dividing the time axis into bins of size, say k, and calculating the probability of spiking in each bin. For a pair of neurons, the cross covariance is estimated in a number of different ways. One of the common estimates is the cross correlogram (also called the covariogram; Nowak and Bullier 2000). Consider several realizations of spike trains from ith and jth neurons. In our case, we only need to estimate $P_{ij}(u)$ since we are considering zero-mean processes (consequently $P_i = P_j = 0$). Initially, we divide the time axis into bins of size, say k. We call one neuron, say jth neuron, as the reference neuron. Consider the first trial. We set time to be zero when the reference neuron spikes for the first time. Then we bin the spikes from the ith neuron with respect to the new shifted time scale. Let D denote the binned data vector. Next we set time to be zero when the jth neuron spikes for the second time and again repeat the process of binning the spikes from the ith neuron. We add this binned data vector to D. We repeat the procedure till we reach the last spike of the jth neuron. Thus the rth element of the final vector D is the value of $dN_i(t+rk)\,dN_j(t)$ for one realization. Taking the mean of vector D over different realizations or trials gives us an estimate of $E\{dN_i(t+rk)\,dN_j(t)\}$ and when plotted as histogram, it is called the cross correlogram between neuron i and neuron j (with jth neuron as reference).

2.2 Spectral representation of point processes

The power spectrum $S_{ii}(f)$ for the process $N_i(t)$ can be defined as the Fourier transform of the auto-covariance density (Bartlett 1963):

$$S_{ii}(f) = \frac{P_i}{2\pi} + \frac{1}{2\pi} \int_{-\infty}^{\infty} \exp(-i2\pi f u) q_{ii}(u) du. \tag{7}$$

As $f \to \infty$, $S_{ii}(f)$ tends to $P_1/2\pi$ (the spectrum of a Poisson process). Similarly, the cross-spectrum $S_{ij}(f)$ between the processes N_i and N_j is defined as the Fourier transform of the cross-covariance density (Bartlett 1963):

$$S_{ij}(f) = \frac{1}{2\pi} \int_{-\infty}^{\infty} \exp(-i2\pi f u) q_{ij}(u) du \tag{8}$$

where $i \neq j$. The spectral matrix for the multivariate point process $N(t)$ is:

$$\mathbf{S}(f) = \begin{pmatrix} S_{11}(f) & ... & S_{1p}(f) \\ ... & ... & ... \\ S_{p1}(f) & ... & S_{pp}(f) \end{pmatrix} \tag{9}$$

with diagonal terms representing auto-spectra and off-diagonal term cross-spectra.

The spectral matrix from a multivariate spike train of length T can be estimated using the multitaper method (Thomson 1982; Jarvis and Mitra 2001; Walden 2000). We start by applying K data tapers $\{h_k\}_{k=1}^{z}$, one after the other, to the ith channel spike train data and taking the Fourier transform:

$$\widetilde{N}_i(f,k) = \int_0^T h_k(t) \exp(-i2\pi f t) dN_i(t)$$

$$= \sum_j h_k(t_j) \exp(-i2\pi f t_j) \tag{10}$$

where $\int_0^T h_k(t)^2 dt = 1$. In the multitaper method, the set of K orthogonal data tapers used (given by the discrete prolate spheroidal sequences) are optimal in that they have good leakage properties. We then obtain estimates for the matrix elements $S_{ij}(f)$ of the spectral matrix using the tapered $\widetilde{N}_1(f)$ in the following expression (Rosenberg et al. 1998)

$$\widehat{S}_{ij}(f) = \frac{1}{2\pi KT} \sum_{k=1}^{K} \widetilde{N}_i(f,k)\widetilde{N}_j(f,k)^*. \tag{11}$$

In case of multiple realizations (trials), Eq. (11) gives an estimate of cross spectrum using one realization. Averaging these estimates over all trials will give the estimate of all the elements of spectral matrix. Note that in case of binned data set, $h_k(t_j)$ in equation (10) is replaced by $h_k(t_j)\eta_j$ where η_j is the number of spikes in the jth bin. While the multitaper method is used here to estimate the spectral density matrix (Mitra and Pesaran 1999), our method will work with the spectral density matrix obtained with any other non-parametric method.

2.3 Granger causality via spectral matrix factorization

For multivariate continuous-valued time series, an autoregressive (AR) model can be fit to the data. From the model one computes the spectral matrix according to

$$\mathbf{S}(f) = \mathbf{H}(f)\Sigma\mathbf{H}^*(f) \tag{12}$$

where $\mathbf{H}(f)$ is the transfer function which depends on the coefficients of the AR model, Σ is the covariance matrix of the error terms in the AR model, and * denotes matrix transposition and complex conjugate (Ding et al. 2000, 2006). The three entities in Eq. (12) are the basis for estimating Granger causality in the spectral domain (Geweke 1982, 1984). For point processes, the spectral matrix $\mathbf{S}(f)$ is estimated from data using Eq. (11). To compute Granger causality we still require the other two entities in Eq. (12). These can be obtained by applying spectral matrix factorization (Wilson 1972) which decomposes $\mathbf{S}(f)$ into a unique corresponding transfer function

$\mathbf{H}(f)$ and the noise covariance matrix $\mathbf{\Sigma}$ (Dhamala et al. 2008a, b).

Now we are in a position to compute Granger causality for point processes. First, consider two spike trains represented by the point processes $N_i(t)$ and $N_j(t)$. We start with the 2×2 spectral submatrix formed by taking the appropriate entries from the overall spectral matrix in Eq. (9). After spectral factorizing this 2×2 spectral matrix, Granger causality from $N_j(t)$ to $N_i(t)$ at frequency f is given by (Ding et al. 2006):

$$I_{N_j \to N_i}(f) = \ln \frac{S_{ii}(f)}{S_{ii}(f) - \left(\Sigma_{jj} - \Sigma_{ij}^2 \big/ \Sigma_{ii} \right) \left| H_{ij}(f) \right|^2}. \quad (13)$$

Reversing i and j gives the Granger causality from $N_i(t)$ to $N_j(t)$. In a system of three or more spike trains, it is often desirable to find out whether a causal influence between any pair of neurons is direct or mediated by others. The above pairwise measure of causality is not able to resolve this issue (Chen et al. 2006b). This has led to the development of the conditional Granger causality (Geweke 1984). The formulations for the frequency domain conditional Granger causality are complex and the reader is referred to Ding et al. (2006) for a complete exposition.

For mathematical simplicity, only two or three interacting neurons are considered above. In fact, the framework can be extended to two or three nonoverlapping groups of interacting neurons, where there is no restriction on the number of neurons in each group. Thus, the method can work, in principle, for any number of neurons in a given recording. In practice, the computational capacity imposes constraints on the maximum number that can be analyzed.

2.4 Assessment of statistical significance

A random permutation procedure (Brovelli et al. 2004) can be used to build a baseline null-hypothesis distribution from which statistical significance is derived. Consider two point processes with many repeated realizations. We can reasonably assume that the data from different realizations are approximately independent of one another. Randomly pairing data for neuron 1 with data for neuron 2 from a different trial leads to the creation of a synthetic ensemble of trials for which there is no interdependence between the two spike trains based on construction, but the temporal structure within a neuron is preserved. Performing such random pairing with many different permutations will result in a distribution of causality corresponding to the null hypothesis of no statistical interdependence. The calculated value from the actual data is compared with this baseline null hypothesis distribution for the assessment of significance levels.

2.5 Summary of the algorithm

A step by step algorithm for computing nonparametric Granger causality from spike train data is given below. A Matlab code implementing this algorithm can be provided to interested readers upon request.

Step 1   The spike trains generated by m neurons are taken as one realization of an m dimensional multivariate stochastic point process denoted by $\mathbf{N}(t)$. The spike trains are binned where the bin width was chosen to be 1 ms for this work. For smaller bin width, many of the bins will contain no spikes, leading to poor estimation of the spectral density matrix.

Step 2   The Fourier transform of $\mathbf{N}(t)$ is estimated using Eq. (10).

Step 3   The spectral density matrix $\mathbf{S}(f)$ for the stochastic process $\mathbf{N}(t)$ is obtained by using Eq. (11).

Step 4   For a given pair of neurons (say, neuron i and neuron j), the spectral submatrix corresponding to this neuron pair is factorized using the spectral factorization algorithm (Wilson 1972; Dhamala et al. 2008a, b), thus giving the decomposition in Eq. (12).

Step 5   Granger causality from neuron j to neuron i is evaluated as a function of frequency by substituting the transfer function $\mathbf{H}(f)$ and the noise covariance matrix $\mathbf{\Sigma}$ in Eq. (13). This function can be examined for frequency characteristics of causal influences or summed over all frequencies to obtain a single time-domain causal influence. A similar procedure is carried out to evaluate causality from neuron i to j.

Step 6   The statistical significance of the causality values obtained above are ascertained using the method of random permutation described above.

Step 7   Steps 4 to 6 is repeated for all neuron pairs of interest. In case of three or more neurons, the conditional Granger causality can also be evaluated.

3 Results

3.1 Simulation

The model neuron has two variables (Izhikevich 2003):

$$\frac{dv}{dt} = 0.04v^2 + 5v + 140 + u - I, \quad (14a)$$

$$\frac{du}{dt} = a(bv - u), \quad (14b)$$

with after-spike resetting (v is reset to c and u is reset to $u+$ d if $v \geq 30$ mV). Here v is the membrane potential of the

neuron, u is a membrane recovery variable, I is the synaptic current or injected DC current, a is the time scale of u, b is the sensitivity of u to subthreshold fluctuations in v, c is the spike reset values of v and d is the spike reset value of u. The values chosen for this study are: $a = 0.2$, $b = 0.2$, $c = -65$ mV, $d = 2$. The input synaptic current I is taken to be a normally distributed random Gaussian variable.

Example 1. Two neurons were coupled in such a way that the output of the first neuron was fed into the second neuron with a time delay of 10 ms, i.e., neuron 1→neuron 2 (see Fig. 1). The output spike train data was modeled as a bivariate point processes $N_1(t)$ and $N_2(t)$. Each realization was 1s in duration. A total of one hundred realizations were simulated. The mean firing rate for the driver neuron (i.e. neuron 1) is 15.93 spikes per second and for the driven neuron (i.e. neuron 2) is 8.33 spikes per second. These firing rates are consistent with those typically found in thalamic and cortical neurons. The spectral matrix was estimated using the multitaper method. The pairwise Granger causality spectra were derived after the spectral matrix factorization procedure and shown in Fig. 2. The causal influence from neuron 1 to neuron 2 is high while there is no corresponding driving from neuron 2 to neuron 1. This is in agreement with model construction. As no specific meaning is assigned to frequency, the time domain Granger causality is used henceforth which is obtained by integrating spectral causality over the entire frequency domain. Table 1 displays the integrated time-domain values. The significance of these values (at the 10% significance level) was tested using the random permutation procedure with 1,000 permutations. We found that Granger causality from neuron 1 to 2 is highly significant whereas Granger causality from neuron 2 to 1 is not significant (NS).

Note that, in this example, the probability that a spike in neuron 1 is followed by a spike in neuron 2 after 10 ms is
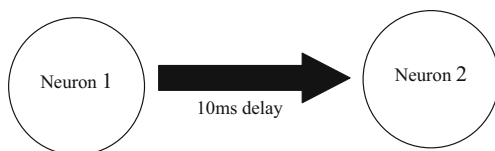

Fig. 1 Schematic diagram depicting the neuronal model in example 1. Neuron 1 drives neuron 2 with a delay of 10 ms. The probability that a spike in neuron 1 is followed by a spike in neuron 2 with 10 ms delay is 0.004

0.004. Despite this low value, the connectivity pattern is correctly recovered. However, if we increase the firing rate to about 100 spikes per second, this probability has to be greater than 0.1 for the method to work. For a firing rate around 200 spikes per second, the probability needs to be around 0.25.

The same data was also subjected to a cross-correlogram analysis using a bin size of 10 ms (Nowak and Bullier 2000). With neuron 1 as the reference, the cross-correlogram gives a peak value of 5.8 for the bin corresponding to a positive time lag of 10–20 ms, thus implying that neuron 1 drives neuron 2, whereas there is no corresponding peak in the opposite direction (see Fig. 3). This demonstrates that, for this simple example, the directionality information determined by Granger causality is also supported by a cross-correlogram analysis.

Example 2. Generally, the relation between two neurons (e.g. neuron 1 and neuron 2 above) may have three contributing factors: neuron 1→ neuron 2, neuron 2→ neuron 1 and a possible common input (see Fig. 4). The cross-correlogram is expected to fail when the common input is strong while the Granger causality would still be able to recover the correct connection pattern. We tested this idea by simulating the case of common input. Here an unknown source, which is assumed to be not measured, drives both neurons 1 and 2 with a delay of 10 ms. There is no direct causal relation between these two neurons. The cross-correlogram with neuron 2 as reference neuron gives significant peaks in both directions yielding the wrong conclusion that the two neurons are reciprocally coupled. Granger causality analysis does not suffer from this problem and gives the correct result that there is no causal relation between the two neurons.

Example 3. To demonstrate the utility of conditional Granger causality, three spiking neurons were connected in such a way that neuron 1 drives neuron 2 with a delay of 10 ms and neuron 2 in turn drives neuron 3 with the same delay (see Fig. 5). A total of 100 trials each of duration 1s were simulated. The results from a pairwise Granger causality analysis are shown in Table 2. Values that are not significant (NS) at the 10% significance level are so indicated.

From the table a causal influence from neuron 1 to neuron 3 is observed while no such connection was built into the model. This connection is spurious and is due to the mediated influence through neuron 2. To resolve this, conditional Granger causality analysis was applied and the result is shown

Fig. 2 A simulation of two spiking neurons where the first neuron drives the second neuron. Pairwise Granger causality spectra from neuron 1 to neuron 2 and vice versa are shown
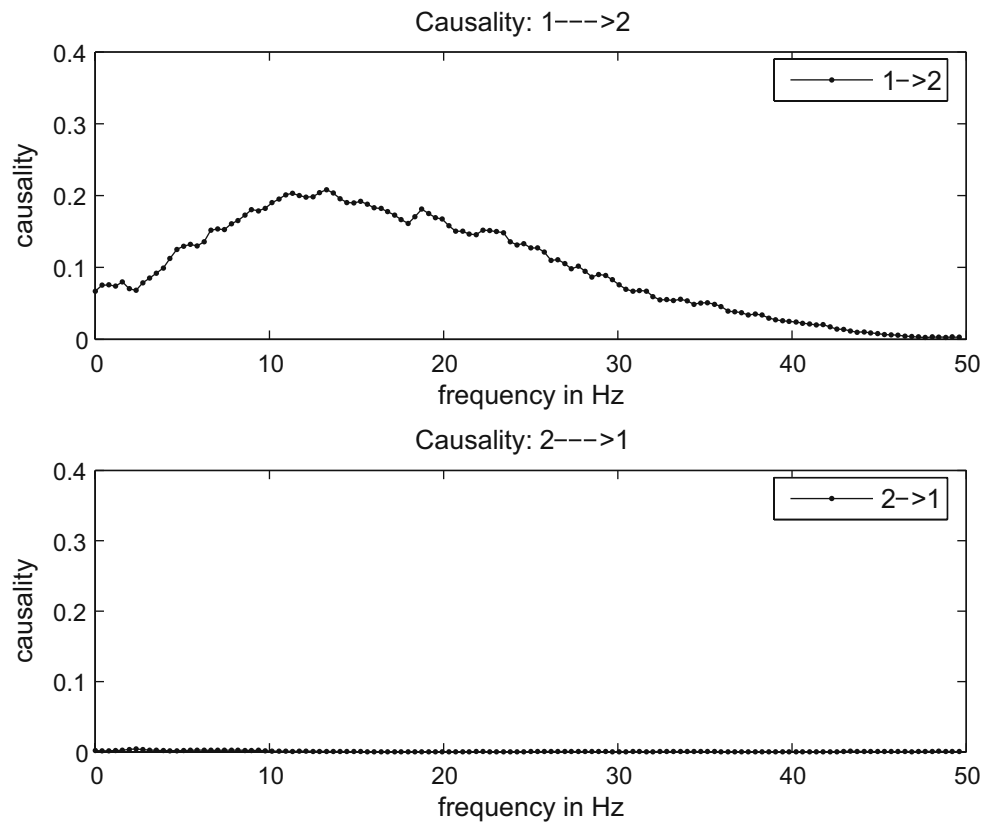
in Table 3. Clearly, when neuron 2 is conditioned out, the causality value from neuron 1 to neuron 3 falls below the significance level. No change in network connectivity is noted from other conditional causality values. Thus the true connectivity pattern is recovered from conditional Granger causality analysis (Chen et al. 2006b; Ding et al. 2006). Such an analysis is not possible with the conventional cross-correlogram technique.

3.2 Experimental data

An array of 16 Teflon coated stainless steel microwires (50 μm uncoated diameter) was implanted in area 3b of an adult squirrel monkey in the hand region such that the wires spanned representations of digit 2 to digit 5. In addition, a bundle of 16 wires was implanted in the ventroposterior lateral (VPL) nucleus of the ipsilateral thalamus. All animal procedures were approved by the Institutional Animal Care

and Use Committee and followed NIH guidelines. The receptive fields of the neurons recorded from the VPL spanned from digit 3, digit 4, digit 5, palm and wrist on the forelimb to parts of the leg and foot (including toes) on the lower limb. Single neuron activity was recorded simulta-
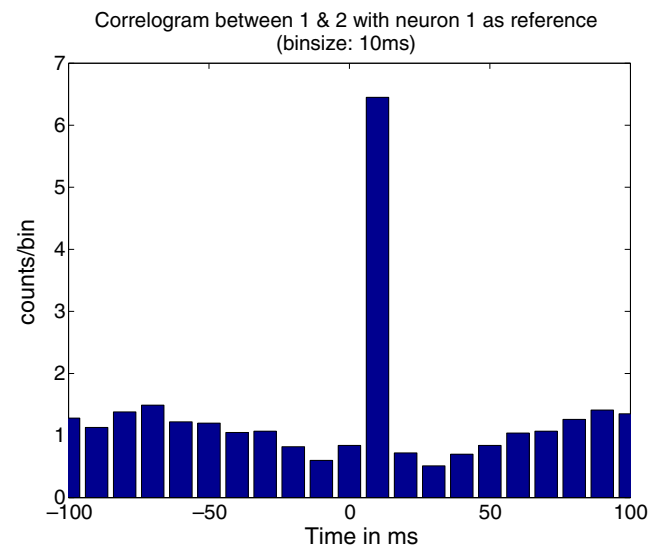

Fig. 3 Crosscorrelogram between neuron 1 and neuron 2 with neuron 1 as reference neuron. A significant peak is obtained corresponding to 10–20 ms bin showing causal relation from neuron 1 to neuron 2 with a delay between 10–20 ms
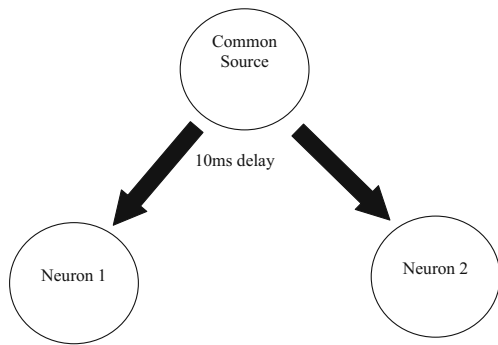
Table 1 Time-domain Granger causality values between neuron 1 and neuron 2 for both directions for example 1

Direction of causality	Causality
1 → 2	25.1082[a]
2 → 1	0.2178

[a] Means statistically significant value

Fig. 4 Schematic diagram depicting the neuronal model in example 2. A common source is driving both neurons with a delay of 10 ms

neously from the cortex and the thalamus (see Jain et al. 2001). The spikes were sorted and recorded using a 32 channel Multichannel Neuronal Acquisition Processor (MNAP) system (Plexon, Dallas, TX). A Chubbuck type stimulator was used to stimulate contralateral radial wrist at 1 Hz for 360 s. The probe contacted the skin for 20 ms in every cycle.

For this study the data from three neurons were considered (two cortical, one thalamic). One cortex–thalamus pair of simultaneously recorded neurons (DSP06a, DSP25a) had overlapping receptive fields and another pair (DSP10a, DSP25a) had nearly disjoint but adjacent receptive fields. The data were epoched into trials triggered on stimulus onset (0 ms). The peristimulus time histograms (PSTH) for all three neurons are shown in Fig. 6. All neurons exhibited brief but vigorous response to stimulus input. The time period 0–30 ms was chosen for Granger causality analysis. The result is shown in the table embedded in Fig. 6. Significant causal influence, at a 10% level of significance, was observed from thalamus to cortex for the neuron pair that had overlapping
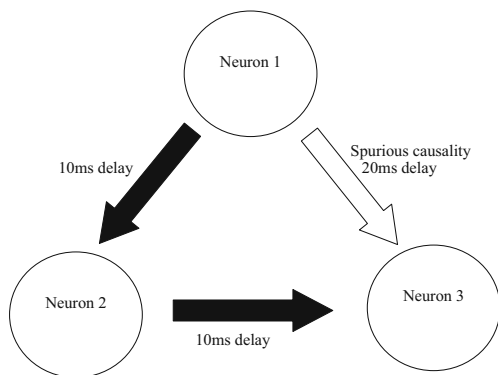

Fig. 5 Schematic diagram depicting the neuronal model in example 3. Here neuron 1 drives neuron 2 with a delay 10 ms and neuron 2 drives neuron 3 with delay of 10 ms. Pairwise analysis yields a spurious causality from neuron1 to neuron 3. The probability that a spike in neuron 1 is followed by a spike in neuron 2 with 10 ms delay is 0.006 and the probability that a spike in neuron 2 is followed by a spike in neuron 3 with 10 ms delay is 0.005

Table 2 Time-domain Granger causality values between distinct pairs of neurons for example 3

Direction of causality	Causality
1 → 2	10.0373[a]
2 → 1	0.0734
1 → 3	0.7986[a]
3 → 1	0.1741
2 → 3	7.9877[a]
3 → 2	0.1251

[a] Means statistically significant value

receptive fields, whereas the causality in the reverse direction (i.e. from cortex to thalamus) was not significant, reflecting a sensory-driven feed forward activation (Kaas et al. 2002). For the neuron pair where the receptive fields sharing a small overlap, the causality was not significant in both directions, a consequence of the somatotopic nature of thalamo-cortical projections (Kaas et al. 2002). These Granger causality results and their physiological and anatomical interpretability provide validation of our nonparametric estimation algorithm in the analysis of actual neural data.

4 Discussion

In neural systems, as in many other systems in science and engineering, analyzing causal relations between recordings from different neurons or different brain sites is of increasing interest. Granger causality has emerged in recent years as a useful empirical method for this purpose. The evaluation of Granger causality could be carried out either in the time domain (Granger 1969; Pierce 1979; Boudjellaba et al. 1992; Goebel et al. 2003; Hesse et al. 2003; Chen et al. 2004; Salazar et al. 2004; Roebroeck et al. 2005) or in the frequency domain (Geweke 1982, 1984; Bernasconi and Konig 1999; Bernasconi et al. 2000; Kaminski et al. 2001; Brovelli et al. 2004; Kus et al. 2004; Chen et al. 2006a, b; Ding et al. 2006; Bollimunta et al. 2008; Zhang et al. 2008). Both time-domain and frequency-domain Granger causality have enabled

Table 3 Time-domain conditional Granger causality values between distinct pairs of neurons (conditioned on the neuron indicated in column 2) for example 3

Direction of causality	Conditioned on	Conditional causality
1 → 2	3	10.0617[a]
2 → 1	3	0.0801
1 → 3	2	0.2016
3 → 1	2	0.1791
2 → 3	1	7.3845*
3 → 2	1	0.1493

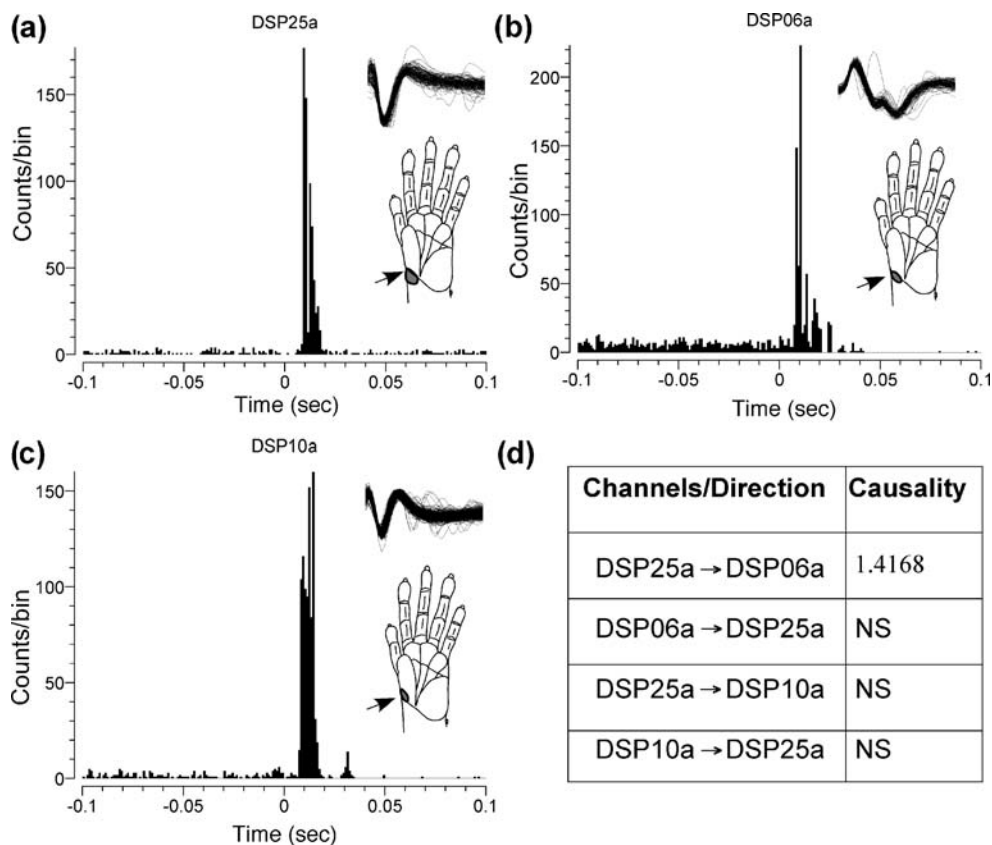[a] Means statistically significant value.

Fig. 6 PSTH of three neurons and the table of Granger causal influences. Granger causality for neuron DSP25a from the ventroposterior (VP) nucleus of thalamus paired with neurons DSP06a or DSP10a from cortical area 3b. All three neurons had receptive fields in the region of radial wrist and the adjacent thenar pad. The receptive fields of neurons DSP25a [see (**a**)] from the VP nucleus and DSP06a (**b**) from area 3b completely overlapped. Responses from 0–30 ms were selected for analysis. Causality was significant from the VP nucleus neuron to the area 3b neuron with overlapping receptive fields [see table in (**d**)]. Causality was not significant in the reverse direction. Neuron DSP10a of area 3b had receptive field on the radial part of proximal thenar pad which is adjacent and partially overlapping with that for DSP06a and DSP25a. Although this neuron is also activated by the stimulus [see (**c**)], causality between the thalamic neuron DSP25a and this neuron was not significant. *Insets* in (**a**–**c**) show the spike waveforms and the receptive fields (*arrows*) of the neurons

insights into sensory and cognitive processing not possible with other methods (Bernasconi and Konig 1999; Bernasconi et al. 2000; Goebel et al. 2003; Hesse et al. 2003; Brovelli et al. 2004; Salazar et al. 2004; Chen et al. 2006b; Ding et al. 2006; Bollimunta et al. 2008; Zhang et al. 2008).

Despite its promise, the Granger causality technique has mainly been applied to continuous-valued time series data, such as EEG and local field potentials. For neuronal spike trains, which are point processes, the present parametric approach used for Granger causality estimation is not directly applicable. In this paper we have proposed a new nonparametric method to compute Granger causality directly from the Fourier transforms of spike train data. Factorization of the spectral matrix and Geweke's spectral domain formulation of Granger causality play a central role in this approach. The main advantage of the proposed method is that it gives both the time-domain and frequency-domain Granger causality while preserving the point-process structure inherent in the data. The method was first validated by

simulated examples where the answer is known, and then applied to experimental recordings to obtain results that were physiologically and anatomically interpretable.

It should be pointed out that the Granger causality method in its present form has two weaknesses: requirement of stationarity and reliance on second-order statistics. While the first weakness may be overcome with a moving window approach, to overcome the second weakness, one needs to incorporate the full conditional density function. The work by Truccolo et al. (2005) provides a framework in that direction and Okatan et al. (2005) used the framework for connectivity analysis.

In closing, we comment that there are other ways of analyzing interaction patterns in multivariate neural data. For example, Okatan et al. (2005) and Truccolo et al. (2005) considered state-space modeling of neural spike trains. By comparing relative estimates of conditional probability density one can achieve the goal of inferring directional information. A different idea based on the information theory has been put forth by Lungarella and Sporns (2006) and

applied to the analysis of sensorimotor networks. The temporal evolution of correlated states using the maximum entropy method was investigated by Tang et al. (2008). These methods and the method proposed in this paper are different in both their initial conceptualization and their framework of estimation. A detailed comparison of each method's performance against well-characterized neurophysiological data would serve to identify their relative strengths and weaknesses.

References

Albo, Z., Di Prisco, G. V., Chen, Y., Rangarajan, G., Truccolo, W., Feng, J., et al. (2004). Is partial coherence a viable technique for identifying generators of neural oscillations? *Biological Cybernetics*, *90*, 318–326. doi:10.1007/s00422-004-0475-5.

Baccala, L. A., & Sameshima, K. (2001). Partial directed coherence: A new concept in neural structure determination. *Biological Cybernetics*, *84*, 463–474. doi:10.1007/PL00007990.

Bartlett, M. S. (1963). The spectral analysis of point processes. *Journal of the Royal Statistical Society B*, *25*, 264–280.

Bernasconi, C., & Konig, P. (1999). On the directionality of cortical interactions studied by structural analysis of electrophysiological recordings. *Biological Cybernetics*, *81*, 199–210. doi:10.1007/s004220050556.

Bernasconi, C., von Stein, A., Chiang, C., & Konig, P. (2000). Bi-directional interactions between visual areas in the awake behaving cat. *Neuroreport*, *11*, 689–692.

Bollimunta, A., Chen, Y., Schroeder, C. E., & Ding, M. (2008). Neuronal mechanisms of cortical alpha oscillations in awake-behaving macaques. *The Journal of Neuroscience*, *28*, 9976–9988.

Boudjellaba, H., Dufour, J., & Roy, R. (1992). Testing causality between two vectors in multivariate autoregressive moving average models. *Journal of the American Statistical Association*, *87*, 1082–1090. doi:10.2307/2290645.

Brillinger, D. R. (1992). Nerve-cell spike train data-analysis—A progression of technique. *Journal of the American Statistical Association*, *87*, 260–271. doi:10.2307/2290256.

Brovelli, A., Ding, M., Ledberg, A., Chen, Y. H., Nakamura, R., & Bressler, S. L. (2004). Beta oscillations in a large-scale sensorimotor cortical network: Directional influences revealed by Granger causality. *Proceedings of the National Academy of Sciences of the United States of America*, *101*, 9849–9854. doi:10.1073/pnas.0308538101.

Brown, E. N., Kass, R. E., & Mitra, P. P. (2004). Multiple neural spike train data analysis: state-of-the-art and future challenges. *Nature Neuroscience*, *7*, 456–461. doi:10.1038/nn1228.

Chen, Y. H., Rangarajan, G., Feng, J. F., & Ding, M. Z. (2004). Analyzing multiple nonlinear time series with extended Granger causality. *Physics Letters Part A*, *324*, 26–35. doi:10.1016/j.physleta.2004.02.032.

Chen, Y., Bressler, S. L., & Ding, M. (2006a). Stochastic modeling of neurobiological time series: Power, coherence, Granger causality, and separation of evoked responses from ongoing activity. *Chaos (Woodbury, N.Y.)*, *16*, 026113. doi:10.1063/1.2208455.

Chen, Y. H., Bressler, S. L., & Ding, M. (2006b). Frequency decomposition of conditional Granger causality and application to multivariate neural field potential data. *Journal of Neuroscience Methods*, *150*, 228–237. doi:10.1016/j.jneumeth.2005.06.011.

Conway, B. A., Halliday, D. M., & Rosenberg, J. R. (1993). Detection of weak synaptic interactions between single Ia-afferent and motor-unit spike trains in decerebrate cats. *The Journal of Physiology*, *471*, 379–409.

Dahlhaus, R., Eichler, M., & Sandkuhler, K. (1997). Identification of synaptic connections in neural ensembles by graphical methods. *Journal of Neuroscience Methods*, *77*, 93–107. doi:10.1016/S0165-0270(97)00100-3.

Daley, D., & Vere-Jones, D. (2003). *An introduction to the theory of point processes, vol. I: Elementary theory and methods*. New York: Springer.

Daley, D., & Vere-Jones, D. (2007). *An introduction to the theory of point processes, vol. II: General theory and structure*. New York: Springer.

Dhamala, M., Rangarajan, G., & Ding, M. (2008a). Estimating Granger causality from Fourier and wavelet transforms of time series data. *Physical Review Letters*, *100*, 018701.1–018701.4.

Dhamala, M., Rangarajan, G., & Ding, M. (2008b). Analyzing information flow in brain networks with nonparametric Granger causality. *NeuroImage*, *41*, 354–362. doi:10.1016/j.neuroimage.2008.02.020.

Ding, M., Bressler, S. L., Yang, W., & Liang, H. (2000). Short-window spectral analysis of cortical event-related potentials by adaptive multivariate autoregressive modeling: data preprocessing, model validation, and variability assessment. *Biological Cybernetics*, *83*, 35–45. doi:10.1007/s004229900137.

Ding, M., Chen, Y., & Bressler, S. L. (2006). Granger causality: Basic theory and applications to neuroscience. In B. Schelter, M. Winterhalder, & J. Timmer (Eds.), *Handbook of Time Series Analysis* (pp. 437–460). Weinheim: Wiley-VCH.

Fanselow, E. E., Sameshima, K., Baccala, L. A., & Nicolelis, M. A. L. (2001). Thalamic bursting in rats during different awake behavioral states. *Proceedings of the National Academy of Sciences of the United States of America*, *98*, 15330–15335. doi:10.1073/pnas.261273898.

Geweke, J. (1982). Measurement of linear dependence and feedback between multiple time series. *Journal of the American Statistical Association*, *77*, 304–313. doi:10.2307/2287238.

Geweke, J. (1984). Measures of conditional linear dependence and feedback between time series. *Journal of the American Statistical Association*, *79*, 907–915. doi:10.2307/2288723.

Goebel, R., Roebroeck, A., Kim, D. S., & Formisano, E. (2003). Investigating directed cortical interactions in time-resolved fMRI data using vector autoregressive modeling and Granger causality mapping. *Magnetic Resonance Imaging*, *21*, 1251–1261. doi:10.1016/j.mri.2003.08.026.

Granger, C. (1969). Investigating causal relations by econometric models and cross-spectral methods. *Econornetrica*, *37*, 424–438. doi:10.2307/1912791.

Halliday, D. M., Rosenberg, J. R., Amjad, A. M., Breeze, P., Conway, B. A., & Farmer, S. F. (1995). A framework for the analysis of mixed time series/point process data-theory and application to the study of physiological tremor, single motor unit discharges and

electromylograms. *Progress in Biophysics and Molecular Biology*, *64*, 237–238. doi:10.1016/S0079-6107(96)00009-0.

Hesse, W., Moller, E., Arnold, M., & Schack, B. (2003). The use of time-variant EEG Granger causality for inspecting directed interdependencies of neural assemblies. *Journal of Neuroscience Methods*, *124*, 27–44. doi:10.1016/S0165-0270(02)00366-7.

Izhikevich, E. M. (2003). Simple model of spiking neurons. *IEEE Transactions on Neural Networks*, *14*, 1569–1572. doi:10.1109/TNN.2003.820440.

Jain, N., Qi, H.-X., & Kaas, J. H. (2001). Long-term chronic multichannel recordings from sensorimotor cortex and thalamus of primates. Prog Brain Res, *130*, 63–72. doi:10.1016/S0079-6123(01)30006-7.

Jarvis, M. R., & Mitra, P. P. (2001). Sampling properties of the spectrum and coherency of sequences of action potentials. *Neural Computation*, *13*, 717–749. doi:10.1162/089976601300014312.

Kaas, J. H., Jain, N., & Qi, H.-X. (2002). The organization of the somatosensory system in primates. In R. J. Nelson (Ed.), *The somatosensory system-deciphering the brain's own body image* (pp. 1–25). New York: CRC.

Kaminski, M., Ding, M., Truccolo, W. A., & Bressler, S. L. (2001). Evaluating causal relations in neural systems: Granger causality, directed transfer function and statistical assessment of significance. *Biological Cybernetics*, *85*, 145–157. doi:10.1007/s004220000235.

Kus, R., Kaminski, M., & Blinowska, K. J. (2004). Determination of EEG activity propagation: Pair-wise versus multichannel estimate. *IEEE Transactions on Bio-Medical Engineering*, *51*, 1501–1510. doi:10.1109/TBME.2004.827929.

Lungarella, M., & Sporns, O. (2006). Mapping information flow in sensorimotor networks. *PLoS Computational Biology*, *2*, 1301–1312.

Mitra, P. P., & Pesaran, B. (1999). Analysis of dynamic brain imaging data. *Biophysical Journal*, *76*, 691–708.

Nowak, L. G., & Bullier, J. (2000). Crosscorrelograms for neuronal spike trains. Different types of temporal correlation in neocortex, their origin and significance. In R. Miller (Ed.), *Time and the Brain: Conceptual Advances in Brain Research* (pp. 53–96). Amsterdam: Harwood Academic.

Okatan, M., Wilson, M. A., & Brown, E. N. (2005). Analyzing functional connectivity using a network likelihood model of ensemble neural spiking activity. *Neural Computation*, *17*, 1927–1961. doi:10.1162/0899766054322973.

Pierce, D. A. (1979). R2 measures for time series. *Journal of the American Statistical Association*, *74*, 901–910. doi:10.2307/2286421.

Roebroeck, A., Formisano, E., & Goebel, R. (2005). Mapping directed influence over the brain using Granger causality and fMRI. *NeuroImage*, *25*, 230–242. doi:10.1016/j.neuroimage.2004.11.017.

Rosenberg, J. R., Amjad, A. M., Breeze, P., Brillinger, D. R., & Halliday, D. M. (1989). The Fourier approach to the identification of functional coupling between neuronal spike trains. *Progress in Biophysics and Molecular Biology*, *53*, 1–31. doi:10.1016/0079-6107(89)90004-7.

Rosenberg, J. R., Halliday, D. M., Breeze, P., & Conway, B. A. (1998). Identification of patterns of neuronal connectivity-partial spectra, partial coherence, and neuronal interactions. *Journal of Neuroscience Methods*, *83*, 57–72. doi:10.1016/S0165-0270(98)00061-2.

Salazar, R. F., Konig, P., & Kayser, C. (2004). Directed interactions between visual areas and their role in processing image structure and expectancy. *The European Journal of Neuroscience*, *20*, 1391–1401. doi:10.1111/j.1460-9568.2004.03579.x.

Sameshima, K., & Baccala, L. A. (1999). Using partial directed coherence to describe neuronal ensemble interactions. *Journal of Neuroscience Methods*, *94*, 93–103. doi:10.1016/S0165-0270(99)00128-4.

Seth, A. K. (2005). Causal connectivity of evolved neural networks during behavior. *Network-Computation in Neural Systems*, *16*, 35–54. doi:10.1080/09548980500238756.

Tang, A., Jackson, D., Hobbs, J., Chen, W., Smith, J. L., Patel, H., et al. (2008). A maximum entropy model applied to spatial and temporal correlations from cortical networks *in Vitro*. *The Journal of Neuroscience*, *28*(2), 505–518. doi:10.1523/JNEUROSCI.3359-07.2008.

Thomson, D. J. (1982). Spectrum estimation and harmonic analysis. *Proceedings of the IEEE*, *70*, 1055–1096. doi:10.1109/PROC.1982.12433.

Truccolo, W., Eden, U. T., Fellows, M. R., Donoghue, J. P., & Brown, E. N. (2005). A point process framework for relating neural spiking activity to spiking history, neural ensemble, and extrinsic covariate effects. *Journal of Neurophysiology*, *93*, 1074–1089. doi:10.1152/jn.00697.2004.

Walden, A. T. (2000). A unified view of multitaper multivariate spectral estimation. *Biometrika*, *87*, 767–788. doi:10.1093/biomet/87.4.767.

Wilson, G. T. (1972). The factorization of matricial spectral densities. *SIAM Journal on Applied Mathematics*, *23*, 420–426. doi:10.1137/0123044.

Wu, J. H., Liu, X. G., & Feng, J. F. (2008). Detecting causality between different frequencies. *Journal of Neuroscience Methods*, *167*, 367–375. doi:10.1016/j.jneumeth.2007.08.022.

Zhang, Y., Chen, Y., Bressler, S. L., & Ding, M. (2008). Response preparation and inhibition: The role of the cortical sensorimotor beta rhythm. *Neuroscience*, *156*, 238–246. doi:10.1016/j.neuroscience.2008.06.061.

Zhu, L., Lai, Y. C., Hoppensteadt, F. C., & He, J. (2003). Probing changes in neural interaction during adaptation. *Neural Computation*, *15*, 2359–2377. doi:10.1162/089976603322362392.